Document downloaded from:

http://hdl.handle.net/10251/160215

This paper must be cited as:

Liberatore, C.; Calabuig-Serna, A.; Rodolfi, M.; Chiancone, B.; Seguí-Simarro, JM. (2019). Phenological phases of flowering in hop (Humulus lupulus L.) and their correspondence with microsporogenesis and microgametogenesis. Scientia Horticulturae. 256:1-6. https://doi.org/10.1016/j.scienta.2019.108639

The final publication is available at

https://doi.org/10.1016/j.scienta.2019.108639

Copyright Elsevier

Additional Information

Phenological phases of flowering in hop (*Humulus lupulus* L.) and their correspondence with microsporogenesis and microgametogenesis

Running head: Microsporogenesis and microgametogenesis in hop

Claudia M. Liberatore[1], Antonio Calabuig-Serna[2], Margherita Rodolfi[1], Benedetta Chiancone[1] and Jose M. Seguí-Simarro[2,*]

[1] Department of Food and Drug, University of Parma, Italy.

[2] COMAV - Universitat Politècnica de València. CPI, Edificio 8E - Escalera I, Camino de Vera, s/n, 46022. Valencia, Spain.

* Corresponding author

Phone: +34963879047

e-mail: seguisim@btc.upv.es

Abstract

Hop (*Humulus lupulus* L.) suffered, as many other crops, a shrinkage of its intraspecific agrobiodiversity. Biotechnological methods of breeding would offer new opportunities to produce improved varieties with interesting phytochemical profiles and adaptable to the challenging conditions of climate change. Doubled haploid (DH) technology could be a useful tool to increase hop agrobiodiversity but, unfortunately, there is a complete lack of information about hop flower biology. For this reason, the main aim of this work is the study of the different phenological phases of flowering in hop and the corresponding developmental stages of microspores/pollen grains contained therein. The results obtained allowed the identification of morphological markers (anther and flower bud length), easy and fast to measure, that would speed up the selection of flower buds containing the highest percentage of vacuolated microspores and young pollen, the stages considered in most species as the most responsive to androgenesis. A further result, derived from the flower bud and anther microscopical observation, evidenced the increase of lupulin glands on bud and anther surface as the bud proceeds in development from microsporogenesis to microgametogenesis.

Keywords: anther length; bud length; lupulin glands; microspore; pollen; flower development.

Abbreviations

DIC: Differential Interference Contrast

DH: Doubled haploid

Introduction

Hop (*Humulus lupulus* L.) is a dioecious, anemophylus species belonging to the Cannabaceae family. In recent times, increasing demand of craft beers with innovative flavors and the widening of beer consumption (Barth-Hass, 2016) has resulted in a greater general attention for hop culture, and in particular, in the research of hop characterized by peculiar phytochemical profiles. This adds to the need for adaptation of this crop to the challenging conditions of climate change, as it happens for other beer ingredients such as barley (Xie *et al.*, 2018). Unfortunately, during its domestication, hop suffered from a shrinkage of intraspecific agrobiodiversity (Patzak *et al.*, 2010a; Patzak *et al.*, 2010b), which makes these goals even more challenging. In this context, recent studies revealed the occurrence of different types of aneuploidy and chromosome rearrangements that contribute to segregation distortion, a phenomenon that seriously makes hop breeding difficult (Easterling *et al.*, 2018). To overcome these limitations, we are still far from having the biotechnological toolbox already available for other crops. Although the interest of brewing industry for hop resides in the female flower cones, rich in lupulin glands with bitter compounds, males are essential for breeding new hop varieties, as well as for developing advanced biotechnology-based breeding tools.

One of these tools is DH technology. In general, high yields in intensive horticulture are based on the use of hybrids between homozygous (pure) lines. Pure lines are traditionally obtained through classical techniques of self-fertilization and selection, which involves many years of work and important economic investments. As a much faster and cheaper alternative, pure lines can also be generated by DH technology. DHs

are derived from haploid microspores reprogrammed towards embryogenesis. This reduces the process to a single generation, with huge savings of time and economic resources. These advantages make DHs a very interesting tool for breeding companies, which already use them in those crops where the technology is available. Therefore, the development of a reliable protocol for DH production in hop would be a powerful tool to speed up applied hop breeding. However, it is really surprising that, to the best of our knowledge, there is nothing published about DH production in hop. This means that in order to develop such a DH method, we must start from the very beginning, which is the understanding of hop male flower, microspore and pollen development, and its particularities. Unfortunately, there is not much information about microsporogenesis and microgametogenesis. Neither the classical studies of Ehara, (1955, 1956) on hop morphology and development nor the extensive study of Shephard *et al.*, (2000) on hop flower development covered microspore and pollen formation. Only some palynological data are available, which define hop pollen grains as ~20 µm in size, circular to ovate with very thin and scabrate exine, and triporate, with slightly protrusive 2 µm pori that form a subtle annulus (Berger, 2018). Intine is also very thin, although it thickens beneath pores, forming an oncus.

The most efficient way to produce DHs is the experimental induction of androgenesis *in vitro*, either by anther culture or by isolation and culture of microspores in liquid medium. This can only be achieved in a narrow developmental window during microsporogenesis and microgametogenesis. In particular, this window is restricted, in all known species, to the transition from vacuolated microspores to young, bicellular pollen grains (Seguí-Simarro, 2010). Therefore, the first step to develop a DH protocol in hop would be to characterize male flower development, and to find morphological

and easily measurable parameters to identify flower buds and anthers with microspores/pollen at the right developmental window. In this work, we present a study of male hop flower development, characterizing buds, anthers and microspores/pollen at all developmental stages from meiocytes to mature pollen, which would correspond to stages 8-10 of hop male flower development according to Shephard et al., (2000). Based on this study, we propose a criterion to identify the buds containing microspores at the inducible stages, in order to maximize the efficiency of further *in vitro* anther or microspore culture. In order to check the influence of genotype in the measured parameters, this study has been carried out in parallel in three different hop Italian genotypes. To the best of our knowledge, this is first study that reports, firstly, the characterization of the microspore/pollen grain developmental stages in hop, but also that exists a clear correlation between hop microspore/pollen grain developmental stage and male flower bud/anther size. Then, the results presented herein would represent the first step towards the establishment of the optimal parameters to initiate androgenesis induction in hop.

Materials and methods

Plant material

Male flowers were isolated from three hop accessions (MA1, Prismi 2, Santa Clara). Donor plants were grown in the collection field of Manaro sul Panaro (Modena, Italy) during 2018. Plants bloomed and samples were taken in July 2018.

Characterization of flower bud, anther, microspore and pollen development

In order to study the parallel development of microspore/pollen grains and anthers, 20 flower buds per genotype were selected. 50 anthers were randomly isolated, measured from the filament insertion to the apical end with a stereomicroscope equipped with a calibrated eyepiece, separated in dimensional classes, squashed in a glass slide with 10 µl of 7.5 µg/ml 4', 6-diamidino-2-phenylindole (DAPI), and observed with a Zeiss Axiovert 40 CFL inverted microscope. For each anther, the developmental stage of 200 randomly chosen microspores/pollen grains was determined. Data collected were used to calculate percentages of each stage with respect to the total. For each genotype the average anther and flower bud lengths were calculated, correlated and a correlation function was built. Finally, in order to confirm the validity of the correlation function, 50 flower buds were measured with the stereomicroscope from the pedicel insertion to the top of the corolla and divided into dimensional classes. For each dimensional class, 20 anthers were isolated and the developmental stage of 200 randomly chosen microspores/pollen grains was determined as described above. Data collected were used to calculate percentages, and images were taken for characterization of microspore and pollen developmental stages. In addition, 50 male flower buds per genotype were observed with a stereomicroscope to evaluate the presence of trichome hairs and lupulin glands on their bud and anther surface.

Results and Discussion

Characterization of microspore and pollen development

First, we studied the parallel development of microspores/pollen grains (Figures 1A-G, A'-G'), anthers (Figures 1A''-G'') and flower buds (Figures 1A'''-G'''), covering from tetrads to mature pollen grains. Tetrads contained four independent microspores still

enclosed within the post-meiotic cell walls (Figures 1A-A'). At this stage, anthers were small (around 0.5 mm length) and green-yellowish (Figure 1A''), buds were also small (around 1 mm), green and fusiform (Figure 1A'''). Young microspores, upon release from the tetrad, were slightly oval and presented a still thin pollen coat and a centrally located nucleus (Figures 1B, B'). Anthers enlarged dramatically, almost doubling its length with respect to the previous stage (Figure 1B''). The increase in size of anthers, however, was not reflected in a similar size increase in buds, which presented a similar, or slightly larger size (Figure 1B'''). Mid microspores (Figures 1C, C') were similar to young microspores in terms of shape and size, the only remarkable difference being the displacement of the nucleus to the cell periphery, as a consequence of the formation of the central vacuole, typical of this stage. Consequently, anthers (Figure 1C'') and buds (Figure 1C''') underwent minimal changes in size, shape and color. At the vacuolated (mature) microspore stage, remarkable changes were observed. Microspores increased in size and adopted a round morphology (Figure 1D). In addition, a thicker microspore coat was evidenced in DIC images. In fluorescence images (Figure 1D'), an increase in autofluorescence of this coat suggested a compositional change as well. DAPI images also evidenced a nucleus closely apposed to the plasma membrane, indicating the imminence of the first pollen mitosis. In parallel, anthers became larger. Buds enlarged too, adopting an oval shape.

The transition of vacuolated microspores to young bicellular pollen grains (Figures 1E, E') involved the formation of a vegetative and a generative cell, defined by different levels of chromatin condensation in their nuclei, as revealed by the different intensity of DAPI staining. Typically, the vegetative nucleus, transcriptionally active during pollen development, presents lower DNA condensation, whereas the generative nucleus,

precursor of the sperm cells and transcriptionally inactive, presents highly condensed DNA. This transition implied no apparent changes in pollen size or shape, but the formation of a thicker and denser pollen coat, thickened at the apertures. It also implied a notable enlargement of anthers, which adopted a pale yellow color (Figure 1E’’), and of flower buds (Figure 1E’’’). The mid bicellular pollen stage was defined by a thickening of the coat at the level of apertures, now visible at DIC (Figure 1F) and fluorescence images (Figure 1F’), a movement of the generative nucleus from the cell periphery to a central position, a transition of anther color from pale yellow to yellow as pollen matures (Figure 1F’’), and a progressive growth of both anthers and flower buds (Figure 1F’’’). At the mature pollen stage, enlarged and densely filled grains were found (Figure 1G). DAPI staining revealed the presence of three nuclei (Figure 1G’), indicative of the occurrence of the second pollen mitosis. Anthers at this stage (Figure 1G’’) were nearly 2 mm long and yellow, indicative of pollen maturity. In turn, flower buds were wider, and the separation between sepals became more evident (Figure 1G’’’), which was indicative of imminent anthesis. Further stages consisted on anthesis and anther dehiscence, with no changes in pollen grains other than desiccation (data not shown).

Development of lupulin glands in anthers and male flower buds

During all the studied stages of flower bud development, buds remained closed, changing from a fusiform (at early stages) to an oval shape, typical of late stages, in agreement with previous studies that described that hop male flowers open only after pollen maturity has been achieved (Shephard *et al.*, 2000). During all these stages, trichome hairs were abundantly observed on their surface, but no changes in abundance or bulk number were noticed. We also observed the presence of lupulin glands on the

bud surface at all stages. However, their presence was scarce at the first stages and increased notably at the transition from vacuolated microspores to pollen grains (arrows in Figures 1A'''-G'''), coinciding with the increase in bud size and the change in shape. We also found lupulin glands on the surface of anthers at all stages. Again, their number and size increased remarkably in the transition from microspores to pollen and onwards. These newly formed lupulin glands appeared only at the interthecal groove region (arrows in Figures 1A''-G''), as previously suggested (Shephard et al., 2000). Lupulin glands produce lupulin, composed by essential oils, bitter acids and polyphenols, that contribute to beer bitterness and flavor. Our observations on lupulin glands confirm the results of Nagel *et al.*, (2008), who measured a significant presence of polyphenols, and specifically, of xanthohumol in hop male flowers. According to our observations, the presence of xanthohumol would be due to the increase in lupulin glands observed on the bud surface, but principally, on the interthecal grooves of anthers.

Morphological markers to identify anthers and buds enriched in vacuolated microspores and young pollen grains

As explained above, male flowers do not open until the end of microgametogenesis. In addition, we did not observe any macroscopic change during the entire process studied, other than size and a slight widening of the flower bud. Therefore, we focused on these changes in order to establish criteria to easily identify buds at the right developmental window to induce androgenesis. In the three accessions studied, young anthers (1.5-1.8 mm) were characterized by a very homogeneous population of meiocytes/tetrads, comprising 100% of the population in two out of three genotypes. However, as soon as microspores were released from tetrads, anther locules presented a coexisting heterogeneous population of microspores at two or three different stages. Heterogeneity,

as is usual for all plant species studied, increased upon gametogenesis, with up to four different stages in the same anther. To identify the intervals containing the microspore/pollen stages most responsive to androgenesis induction (around the first pollen mitosis), we selected those containing mostly vacuolated microspores and young bicellular pollen (bolded rows in Tables 1, 2). In cases where two intervals contained a clear majority of these stages, we selected the range with a majority of vacuolated microspores with respect to young pollen, since they are at a stage immediately prior to mitosis, and would enter it soon, while young pollen would be exiting this stage. MA 1 anthers contained these stages at the 1.6-1.8 mm interval, whereas Prismi 2 contained them at the 1.7-1.9 mm interval and Santa Clara at the 1.8-2.0 mm interval. The slight genotype-dependent discrepancy in bud and anther size stresses the need for this type of studies in each particular genotype, as for other species (Parra-Vega *et al.*, 2013; Salas *et al.*, 2012; Seguí-Simarro and Nuez, 2005).

As seen, anther length increased in parallel to bud length for the three genotypes. Indeed, we plotted the paired bud and anther lengths (Figure 2) and they matched in all cases to a linear model with remarkably high R^2 coefficients (0,9358 for MA 1, 0,9319 for Prismi 2, 0,9009 for Santa Clara). Dioecy implies that male buds contain only anthers. This, together with the fact that buds remain closed up to the mature pollen stage, likely contributes to this high correlation. Since all three genotypes showed the same linear model, it was possible to develop the following correlation function, $y = 0.9643x - 0.4722$, that will be very useful to infer the anther length (y), knowing the flower bud length (x). Finally, by correlating the percentage of microspores at the different developmental stages with flower bud length, the validity of this function was confirmed. Specifically, the flower bud dimensional class containing the highest percentage of vacuolate microspores (2.1-2.3 mm for MA1 and Prismi2; 2.5-2-7 for

Santa Clara; Table 2) corresponded, using the formula mentioned above, to the most suitable anther length (1.6-1.8 mm interval for MA1, 1.7-1.9 mm interval for Prismi2 and 1.8-2 mm interval for Santa Clara). This is positive in order to be able to use both anther and bud length indistinctly as a reliable criterion, since in other species, buds open or stop grow at intermediate stages of microspore/pollen development (Parra-Vega et al., 2013; Salas et al., 2012; Seguí-Simarro and Nuez, 2005), which precludes such use. However, the strong correlation between buds and anther length observed for the three hop genotypes, makes us propose to use exclusively bud length as the criterion to identify the appropriate stages. This would constitute a fast and easily measurable marker for suitable stages. In case of doubt, or as a second confirmation, anther length or the abundant presence of lupulin glands on the anther groove could also be used.

Conclusion

This work is, to the best of our knowledge, the first detailed characterization of the different microspore/pollen stages during hop male flower development. It represents a first step towards the development of DH technology in hop. First of all, a detailed description of male flowers has been provided, with a particular focus on development of microspores and pollen grains and their features. Furthermore, a correlation between microspore/pollen developmental stages and flower bud/anther size was established. We also showed that in the three genotypes studied, vacuolated microspores and young bicellular pollen are contained in anthers with slightly different lengths. By means of microscopical analysis, it was possible to evidence that lupulin glands on buds and anthers surface, increase in parallel to bud and anther development. Thanks to these results, it will be easier and faster to select flower buds containing microspores at the

most suitable stage of development to induce androgenesis. This, in turn, may allow for the development of innovative techniques such as DH technology for hop breeding.

Author contribution

CML and ACS performed all the experimental work required for this study. MR contributed to sample harvesting and preparation, BC helped in sample preparation, analysis of results and writing of the manuscript. JMSS designed the experiments, analyzed the results and wrote the manuscript.

Funding

This work was supported by Spanish MINECO [grant number AGL2017-88135-R to JMSS] jointly funded by FEDER.

Declarations of interest: none

References

Barth-Hass, G., 2016. The Barth Report, Nuremberg, Germany.

Berger, U.E., 2018. Pollen Atlas. www.pollenwarndienst.at - Medical University of Vienna.

Easterling, K., Pitra, N., J. Jones, R., G. Lopes, L., R. Aquino, J., Zhang, D., D. Matthews, P., Bass, H., 2018. 3D Molecular Cytology of Hop (Humulus lupulus) Meiotic Chromosomes Reveals Non-disomic Pairing and Segregation, Aneuploidy, and Genomic Structural Variation. Front Plant Sci 9, 1501.

Ehara, K., 1955. Comparative Morphological Studies On The Hop (*Humulus Lupulus* L.) And The Japanese Hop (*H. Japonicus* Sieb. ET ZUCC.). I. Journal of the Faculty of Agriculture, Kyūshū University 10, 209-232.

Ehara, K., 1956. Comparative Morphological Studies On The Hop (*Humulus Lupulus* L.) And The Japanese Hop (*H. Japonicus* Sieb. ET ZUCC.). II. Journal of the Faculty of Agriculture, Kyūshū University 10, 307-324.

Nagel, J., Culley, L.K., Lu, Y., Liu, E., Matthews, P.D., Stevens, J.F., Page, J.E., 2008. EST Analysis of Hop Glandular Trichomes Identifies an O-Methyltransferase That Catalyzes the Biosynthesis of Xanthohumol. Plant Cell 20, 186-200.

Parra-Vega, V., González-García, B., Seguí-Simarro, J.M., 2013. Morphological markers to correlate bud and anther development with microsporogenesis and

microgametogenesis in pepper (*Capsicum annuum L.*). Acta Physiol. Plant. 35, 627-633.
Patzak, J., Nesvadba, V., Henychová, A., Krofta, K., 2010a. Assessment of the genetic diversity of wild hops (*Humulus lupulus* L.) in Europe using chemical and molecular analyses. Biochemical Systematics and Ecology 38, 136-145.
Patzak, J., Nesvadba, V., Krofta, K., Henychova, A., Marzoev, A.I., Richards, K., 2010b. Evaluation of genetic variability of wild hops (*Humulus lupulus* L.) in Canada and the Caucasus region by chemical and molecular methods. Genome 53, 545-557.
Salas, P., Rivas-Sendra, A., Prohens, J., Seguí-Simarro, J.M., 2012. Influence of the stage for anther excision and heterostyly in embryogenesis induction from eggplant anther cultures. Euphytica 184, 235-250.
Seguí-Simarro, J.M., 2010. Androgenesis revisited. Bot. Rev. 76, 377-404.
Seguí-Simarro, J.M., Nuez, F., 2005. Meiotic metaphase I to telophase II is the most responsive stage of microspore development for induction of androgenesis in tomato (*Solanum lycopersicum*). Acta Physiol. Plant. 27, 675-685.
Shephard, H.L., Parker, J.S., Darby, P., Ainsworth, C.C., 2000. Sexual development and sex chromosomes in hop. New Phytol. 148, 397-411.
Xie, W., Xiong, W., Pan, J., Ali, T., Cui, Q., Guan, D., Meng, J., Mueller, N.D., Lin, E., Davis, S.J., 2018. Decreases in global beer supply due to extreme drought and heat. Nature Plants 4, 964-973.

Tables

Table 1. Distribution of the stages of microspore/pollen development at different lengths, during anther development in MA 1, Prismi 2 and Santa Clara. The number of microspores/pollen grain units counted at each stage is expressed as the mean ± s.d. of the percentages of total counted microspores/pollen grains. M+T: meiocytes + tetrads; YM: young microspores; MM: mid microspores; VM: vacuolated microspores; YP: young pollen grains; MP: mid pollen grains; LP: late (mature) pollen grains. The bolded row represents the anther length where a majority of vacuolated microspores can be found.

MA 1

Anther length (mm)	M+T	YM	MM	VM	YP	MP	LP
1.0-1.2	90.5±7.4	9.5±7.4					
1.3-1.5		49.5±14.47	33.2±8.3	17.4±7.2			
1.6-1.8			**6.4±3.7**	**73.2±8.4**	**20.4±12.0**		
1.9-2.1			3.0±0.5	12.8±0.5	84.2±0.0		
≥2.2				12.4±1.1	64.6±0.7	19.0±0.8	4.0±1.3

Prismi 2

Anther length (mm)	M+T	YM	MM	VM	YP	MP	LP
1.1-1.3	100±0						
1.4-1.6	61.9±15.6	32.4±12.3	5.7±3.3				
1.7-1.9			**18.3±7.5**	**60.8±13.3**	**20.9±12.3**		
≥2			0.8±0.5	7.0±3.1	70.9±4.5	19.9±5.2	1.5±0.9

Santa Clara

Anther length (mm)	M+T	YM	MM	VM	YP	MP	LP
1.1-1.3	100±0						
1.5-1.7		39.1±16.9	32.1±10.2	28.8±13.2			
1.8-2.0			**1.3±0.3**	**85.0±11.3**	**13.7±11.6**		
2.1-2.3			0.8±0.0	34.1±1.1	65.1±1.0		
>2.4				12.3±0.1	58.0±0.5	27.7±0.4	2±0.2

Table 2. Distribution of the stages of microspore/pollen development at different lengths, during bud development in MA 1, Prismi2 and Santa Clara. The number of microspores/pollen grain units counted at each stage is expressed as the mean ± s.d. of the percentages of total counted microspores/pollen grains. M+T: meiocytes + tetrads; YM: young microspores; MM: mid microspores; VM: vacuolated microspores; YP: young pollen grains; MP: mid pollen grains; LP: late (mature) pollen grains. The bolded row represents the bud length where a majority of vacuolated microspores can be found.

MA 1

Bud length (mm)	M+T	YM	MM	VM	YP	MP	LP
1.5-1.7	82.5±20.3	17.5±10.1					
1.8-2.0		52.1±19.2	20.9±9.0	27±14.3			
2.1-2.3				**80.0±1.2**	**20.0±1.2**		
2.4-2.6				34.5±18.7	65.5±18.7		
≥2.6				12.4±0.7	65.1±0.7	18.6±0.8	430±0.8

Prismi 2

Bud length (mm)	M+T	YM	MM	VM	YP	MP	LP
1.5-1.7	100±0						
1.8-2.0	34.1.±23.6	51.9±18.3	11.2±3.9	2.8±1.6			
2.1-2.3			**8.4±1.5**	**78.3±5.6**	**13.3±7.1**		
≥2.4			9.1±6.6	16.3±7.6	59.5±10.1	13.9±6	1.3±0.8

Santa Clara

Bud length (mm)	M+T	YM	MM	VM	YP	MP	LP
1.6-1.8	100±0						
1.9-2.1	47.8±27.7	48.0±25.3	4.2±2.8				
2.2-2.4		9.8±5	37.9±12.8	52.3±17.0			
2.5-2.7			**1.3±0.3**	**85.0±11.3**	**13.7±11.6**		
>2.8			0.4±0.2	23.2±6.3	61.6±2.1	13.9±8	1±0.6

Figure legends

Figure 1. Changes during microspore/pollen (A-G: DIC images; A'-G': DAPI staining), anther (A''-G''), and bud development (A'''-G''') in hop accession MA 1. A-A''': meiocytes and tetrads. B-B''': Young microspores. C-C''': Mid microspores. D-D''': Vacuolated microspores. E-E''': Young bicellular pollen. F-F''': Mid pollen. G-G''': Mature pollen. ap: aperture; ex: exine microspore/pollen coat; gn: generative nucleus; n: nucleus; s: sperm cell; vn: vegetative nucleus. Arrows point to lupulin glands on the surface of anthers and flower buds. Bars in A-G and A'-G': 10 µm; A''-G'' and A'''-G''': 1 mm.

Figure 2. Correlation between anther and flower bud length in hop male buds of MA 1 (A), Prismi 2 (B) and Santa Clara (C). A regression line and the corresponding R^2coefficient are shown.

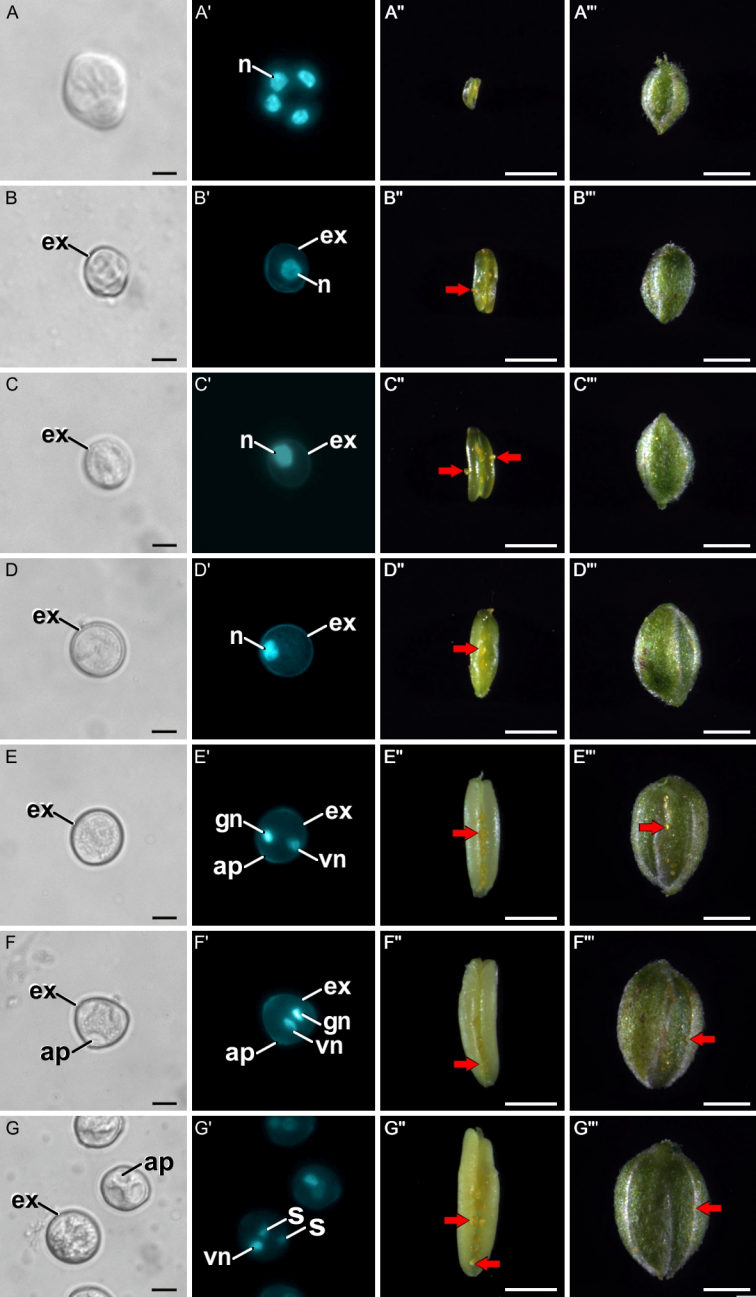
A
A'
n
A"
A"'
B
ex
B'
ex
n
B"
B"'
C
ex
C'
n
ex
C"
C"'
D
ex
D'
n
ex
D"
D"'
E
ex
E'
gn
ex
ap
vn
E"
E"'
F
ex
ap
F'
ex
gn
ap
vn
F"
F"'
G
ap
ex
G'
S
S
vn
G"
G"'

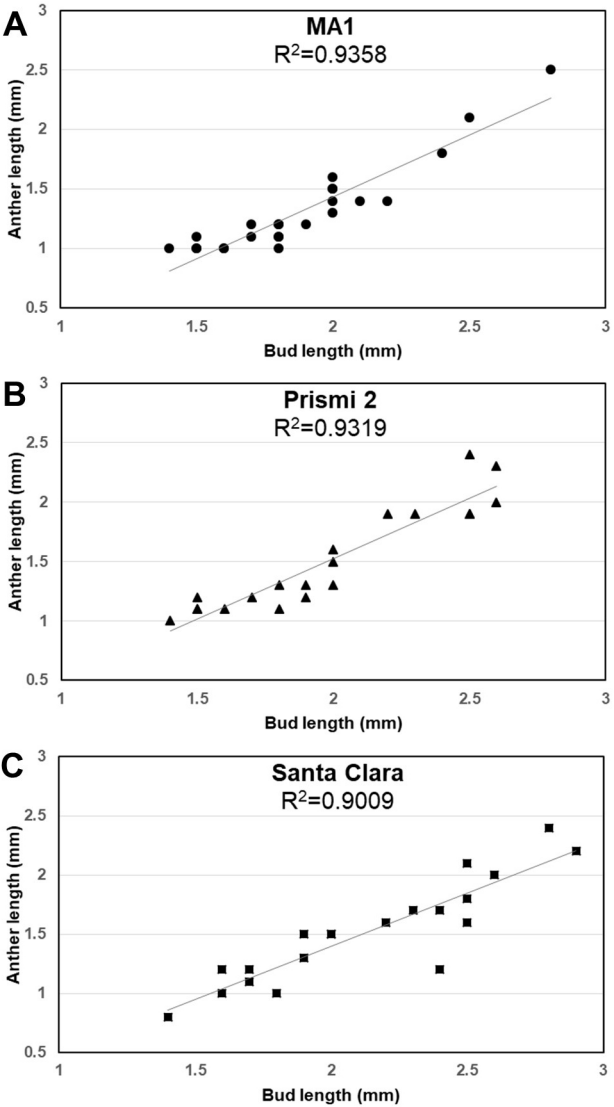
A
MA1
R2=0.9358
Anther length (mm)
Bud length (mm)
B
Prismi 2
R2=0.9319
Anther length (mm)
Bud length (mm)
C
Santa Clara
R2=0.9009
Anther length (mm)
Bud length (mm)